SSRG International Journal of Electrical and Electronics Engineering
ISSN: 2348-8379/ https://doi.org/10.14445/23488379/IJEEE-V12I9P120

Volume 12 Issue 9, 193-201, September 2025
© 2025 Seventh Sense Research Group®

Original Article

Miniaturized Flexible Antenna Performance Analysis using Substrate Integrated Waveguide (SIW)

Archana Tiwari[1], A.A. Khurshid[2]

[1,2]*Electronics Engineering Department, Shri. Ramdeobaba College of Engineering and Management, Nagpur, India.*

[1]*Corresponding Author : tiwariar@rknec.edu*

Received: 15 July 2025 Revised: 16 August 2025 Accepted: 15 September 2025 Published: 30 September 2025

Abstract *- The proposed compact Rectangular Microstrip Antenna (RMSA) design embedded with a Substrate Integrated Waveguide (SIW) is presented. In order to achieve significant miniaturisation without sacrificing performance, the antenna was designed using a flexible textile substrate (εr = 2.75, thickness = 1.5 mm). The implications of adding SIW structure to flexible microstrip antennas were thoroughly examined in this paper. SIW's impact on patch antennas depends on a variety of variables, including the number, diameter, position, and spacing. An investigation was conducted to investigate the effect of altering the diameter, quantity, and placement of vias utilised for SIW. The findings show that SIW integrated into an antenna can drastically reduce its size without sacrificing performance. Additionally, the results demonstrate that multifrequency functioning, better impedance matching, and less cross-polarization may all be achieved by optimising SIW setups. The suggested design is straightforward, small (λ/7), and appropriate for on-body usage in a range of situations.*

Keywords *- RMSA, Antenna, SIW, Flexible, Textile, Compact, Miniaturize.*

1. Introduction

The Rectangular Microstrip Patch Antenna (RMPA), with its remarkable performance, small size, and mobility, has become an essential part of contemporary wireless communication systems. It can be easily integrated into a variety of devices, such as Internet of Things (IoT) devices and wearable technology, due to its versatility and configurability. Innovative processes used for miniaturization enable the RMPA's design to be used for applications with limited space. The performance analysis of an RMPA, which is affected by several electrical and physical factors, is proposed in this paper. Optimising the antenna's performance requires understanding the intricate relationships between these parameters. Through carefully adjusting these variables, designers can customise the antenna's behaviour to satisfy application needs, such as higher gain, wider bandwidth, or smaller dimensions. The miniaturisation of microstrip patch antennas for use in wearable technology has drawn the attention of numerous researchers. For instance, research [1-3] has suggested a wearable, miniature antenna for Wireless Body Area Network (WBAN) uses. The suggested antenna, which operates at 2.45 GHz, was notably reduced in size by 33.3% when compared to traditional patch antennas. This reduction in size was achieved by means of creative design optimisation, demonstrating the possibility of small, powerful antennas in wearable medical equipment. Significant miniaturisation has resulted from recent developments in antenna design, making wearable and small devices possible. A 75% reduction in size without sacrificing performance was accomplished in [4] with a miniaturised textile antenna. The dual-band wearable textile antenna and military beret wearable antenna designs also showed remarkable miniaturisation in [5, 6]. Miniaturisation approaches were further demonstrated by the conformal multiband antenna employing inkjet printing and the compact half-mode substrate-integrated cavity antenna [7, 8]. A novel DRA design with a metasurface achieved a wide impedance bandwidth within a compact footprint [9]. A miniature Van Atta array operating at two frequencies, structured in a two-dimensional configuration for enhanced performance, and compact imaging antennas for EM head imaging systems have demonstrated significant advancements in antenna miniaturization [10-13]. For a variety of new applications, including wearable technology, the Internet of Things, and Wireless Body Area Networks (WBANs), there seems to be a lack of thorough knowledge and methodical approaches for optimising the interaction of several electrical and physical characteristics of Rectangular Microstrip Patch Antennas (RMPAs) in order to concurrently address particular performance metrics (gain, bandwidth, and size). Although much work has been done on miniaturisation for wearable integration, there may be more opportunities to improve RMPA performance for contemporary wireless communication scenarios through careful consideration of parameter trade-offs, application-specific optimisations, and the use of sophisticated design synergies.

This is an open access article under the CC BY-NC-ND license (http://creativecommons.org/licenses/by-nc-nd/4.0/)

2. Antenna Design with Shorting Posts

The rectangular microstrip patch antenna operating in the dominant mode with a resonant length of λ/2 has a full-cycle voltage distribution along its length and zero potential fields in its center. By incorporating SIW structure across the patch width, as discussed in [14, 15], and considering only half the length, a small λ/4-length shorted patch with the same resonant frequency as a λ/2-length rectangular microstrip patch can be designed. Several theoretical approaches, such as Green's function approaches employing cavity models [16, 17] and transmission-line models [18], have been used to evaluate the effects of shorting posts on loading-patch antennas. The dominant mode of the shorted patch structure in the proposed design is the *TM10* mode. Multiple shorting posts or a shorting plate were utilized to conduct a shorting post. Figure 1 depicts the geometry of the proposed design, which features shorting posts spanning the patch's width and a halved patch length. Initially, the resonant length of the rectangular microstrip patch antenna in free space was estimated via Equation (1),

$$L = \frac{0.5\lambda(0)}{\sqrt{\varepsilon(eff)}} \quad (1)$$

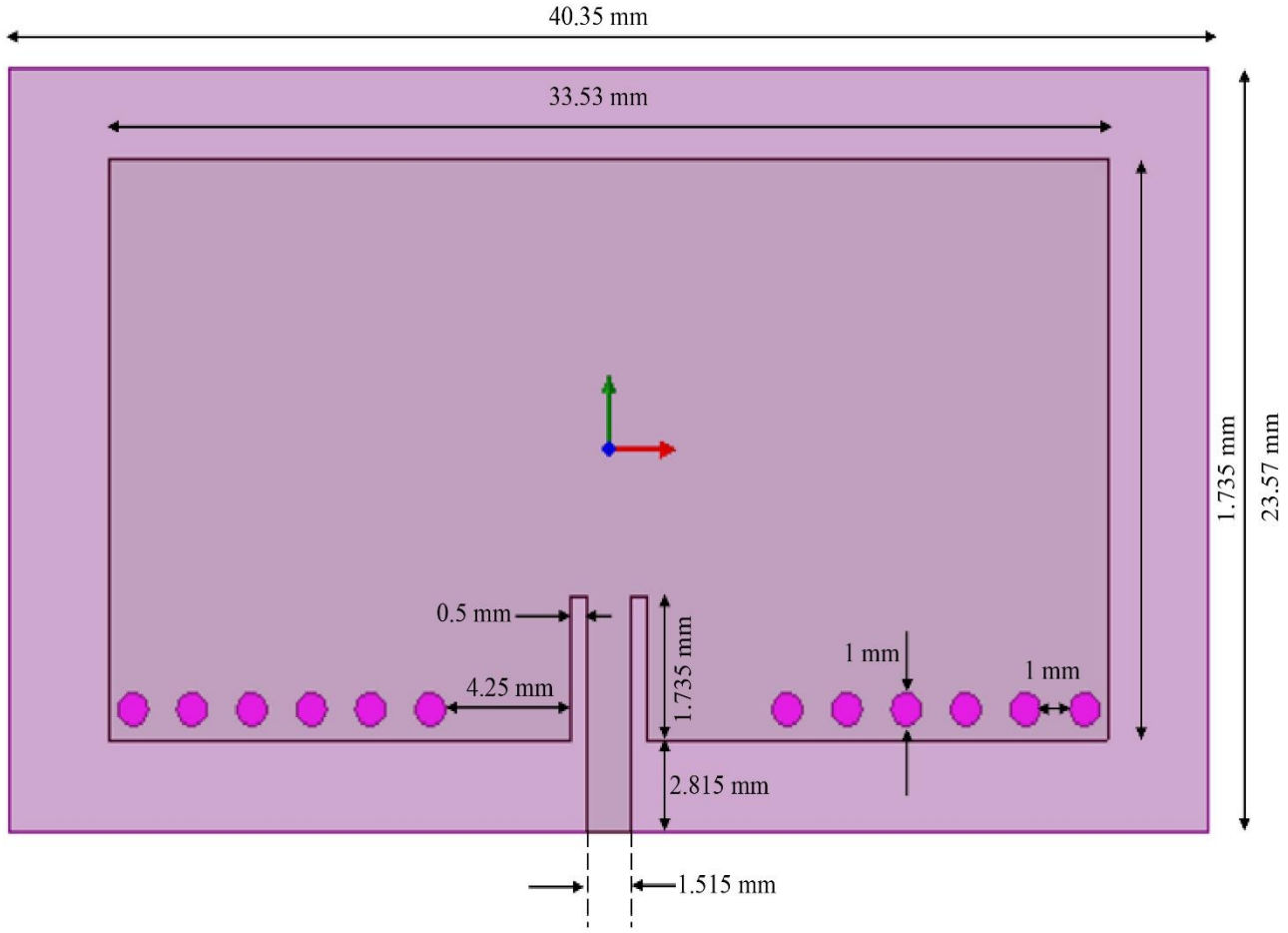

Fig. 1 Geometry of the proposed RMPA design, indicating critical dimensions

Table 1. Comparative analysis of SIW vias variations

Experiment No	Diameter (mm)	Spacing (mm)	Numbers	Frequency (GHz)	|S11| (dB)	Gain (dB)
1	0.5	0.5	36	2.45	15.38	1
2	0.5	0.5	34	2.41	11.88	1
3	0.5	0.5	32	2.37	10.44	1
4	0.5	1	24	2.46	17.54	1
5	0.5	1	22	2.43	17.38	1
6	0.5	1	20	5.65	13.92	1
7	0.5	1	18	5.87	11.22	1
8	0.5	1.5	12	2.41	14.39	1.3

9	0.5	1.5	10	5.53	31.86	1
10	0.5	1.5	8	5.42	11.25	1.3
11	0.5	2	10	2.37	11.35	1.3
12	0.5	2	8	5.5	17.29	1.3
13	1	0.5	16	2.5	13.6	1
14	1	0.5	14	2.46	11.87	1
15	1	0.5	12	2.41	14.55	1
16	1	0.5	10	5.45	13.72	1.3
17	1	1	12	2.46	25.29	1
18	1	1	10	5.56	26.09	1.3
19	1	1	8	5.44	11.83	1.3
20	1	1.5	10	2.46	13.96	1
21	1	1.5	8	5.51	23.76	1.3
22	1	1.5	6	5.37	10.15	1.3
23	1	2	8	2.41 and 5.68	11.56	**1.3**
24	1	2	6	5.45	12.03	1
25	1.5	0.5	12	2.51	20.69	1
26	1.5	0.5	10	5.66	19.79	1
27	1.5	0.5	8	5.44	18.11	1.3
28	1.5	1	10	2.5	20.77	0.9
29	1.5	1	8	5.62	27.29	1
30	1.5	1	6	5.37	10.04	1.1
31	1.5	1.5	8	2.46	14.49	1
32	1.5	1.5	6	5.47	13.17	1.13
33	1.5	2	8	2.5	10.85	0.9
34	1.5	2	6	5.5	25.26	1.13
35	1.5	2	2	5.07	10.03	1.1
36	2	0.5	8	2.54	19.76	0.4
37	2	0.5	6	5.55	15.35	0.8
38	2	1	8	2.58	10.16	0.39
39	2	1	6	5.64	28.89	0.9
40	2	1	4	5.33	10.92	1.1
41	2	1.5	6	2.51	13.01	0.7
42	2	1.5	4	5.4	10.17	0.9
44	2	2	6	2.54	22.16	0.5
45	2	2	4	5.41	11.03	0.9

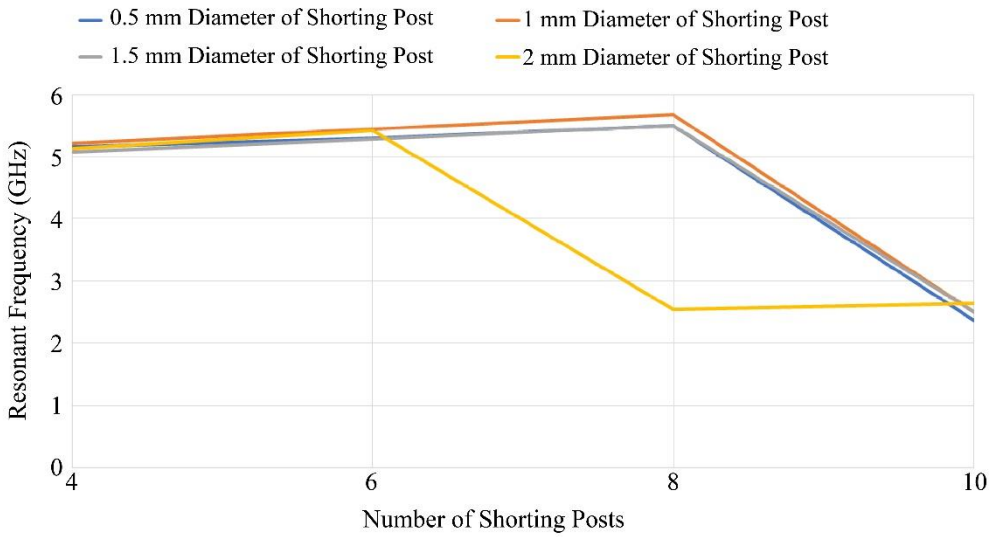

Fig. 2 The resonant frequency response of the antenna for different via counts, with a spacing of 2mm between vias

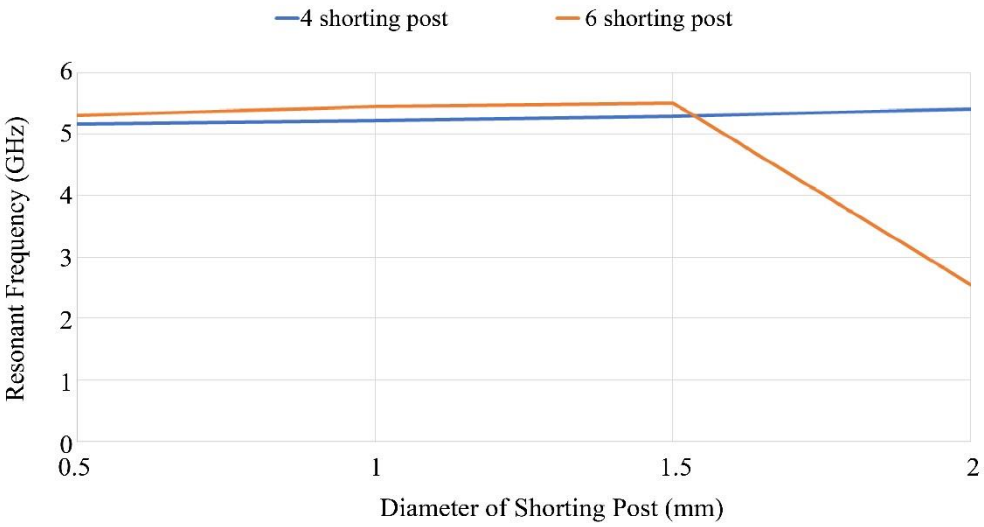

Fig. 3 Resonant frequency of the antenna for variations in the diameter of vias

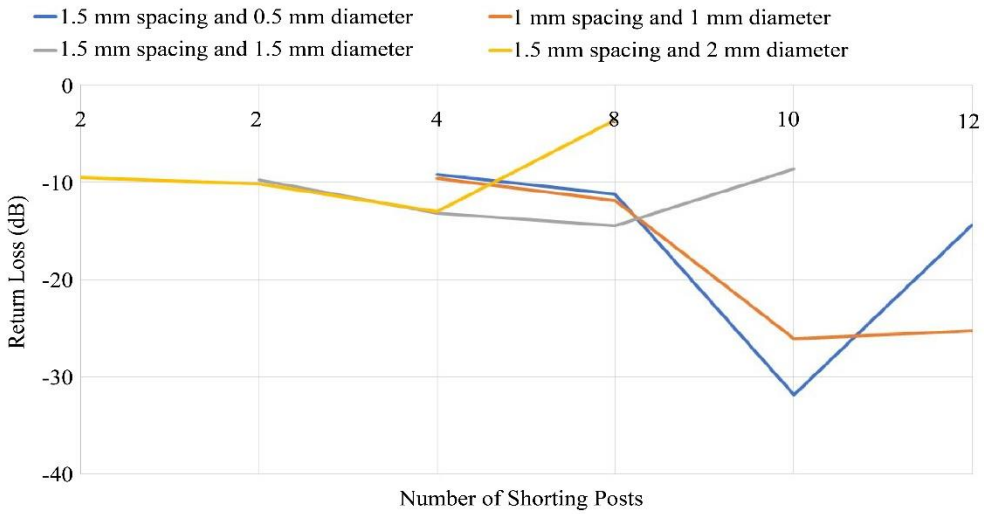

Fig. 4 Reflection coefficient of antenna for variations in the number of vias

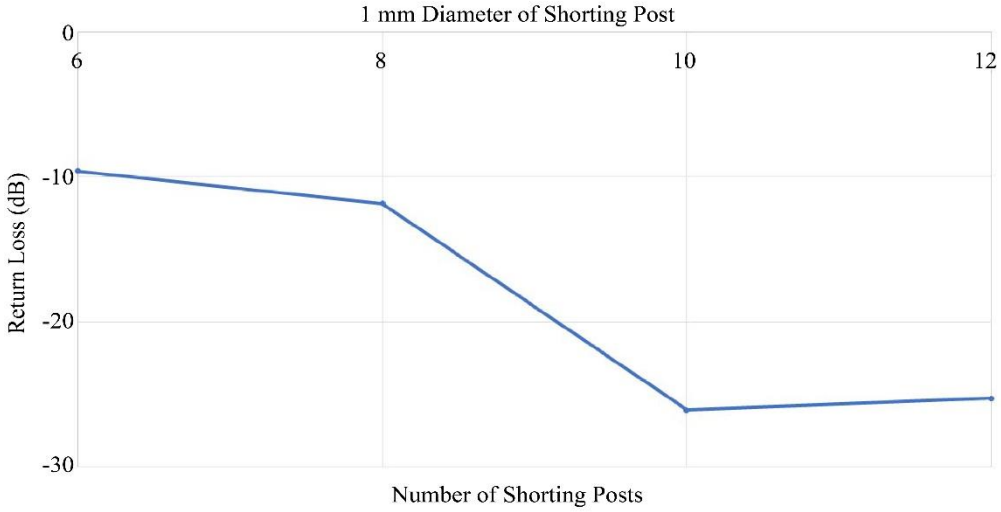

Fig. 5 Return loss for variations in the number of shorting posts

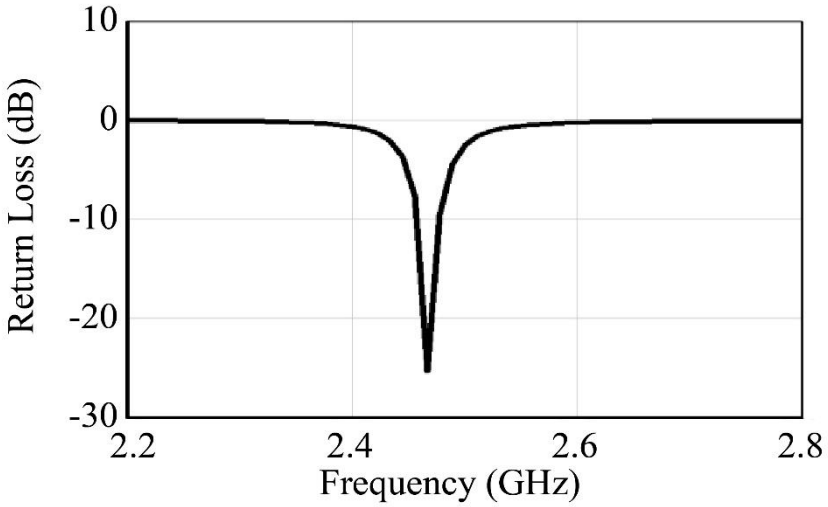

Fig. 6 The miniaturized antenna's |S11| and frequency response plot

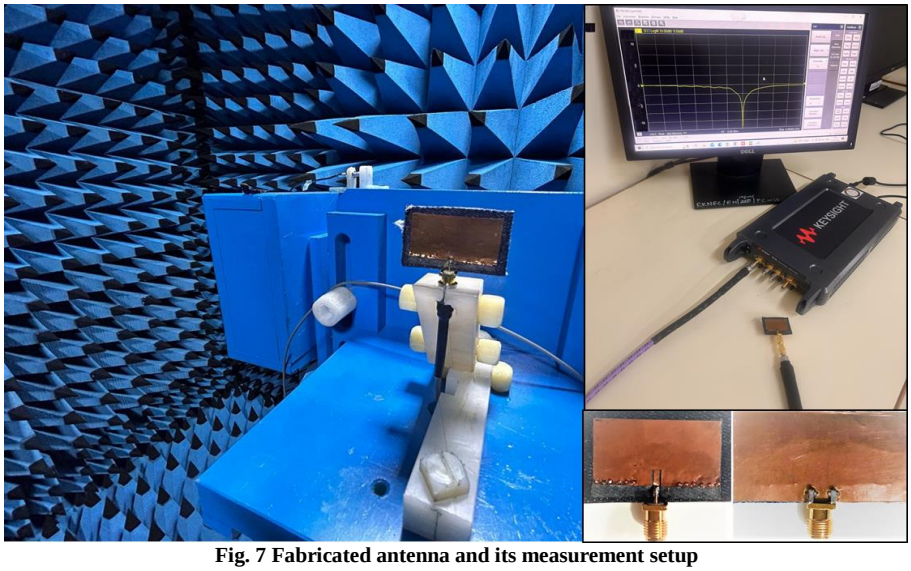

Fig. 7 Fabricated antenna and its measurement setup

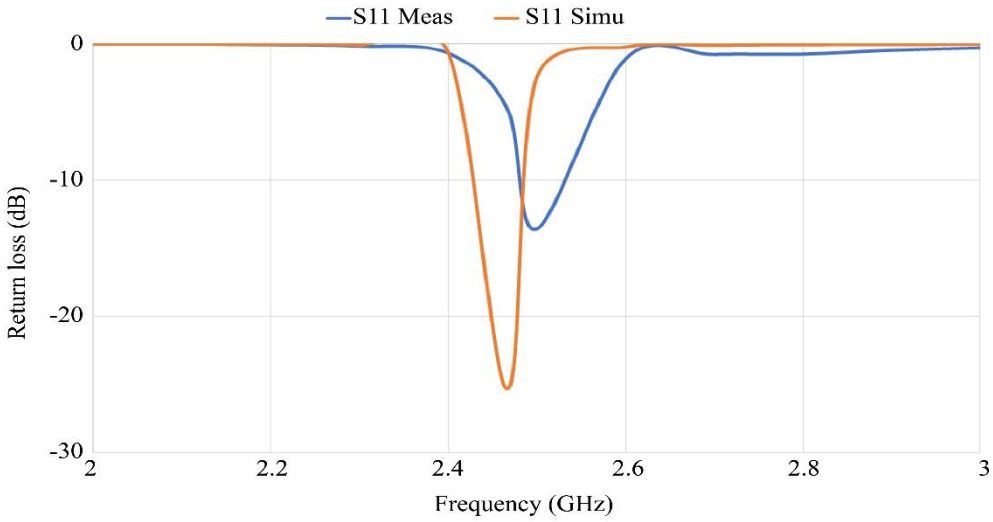

Fig. 8 A plot comparing simulated and measured return loss as a function of frequency

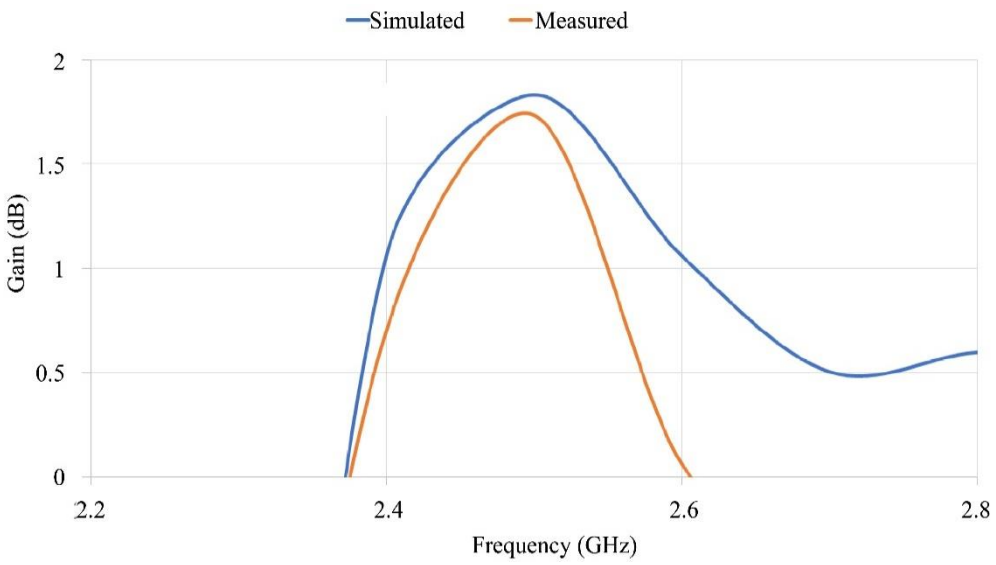

Fig. 9 Simulated and measured gain vs. frequency plot

Table 2. Simulated & measured results of the antenna

Parameters	Frequency	|S11|	Gain
Data obtained through simulation	2.46 GHz	25.29 dB	1 dB
Data obtained through measurement	2.5 GHz	13.6 dB	1.73 dB

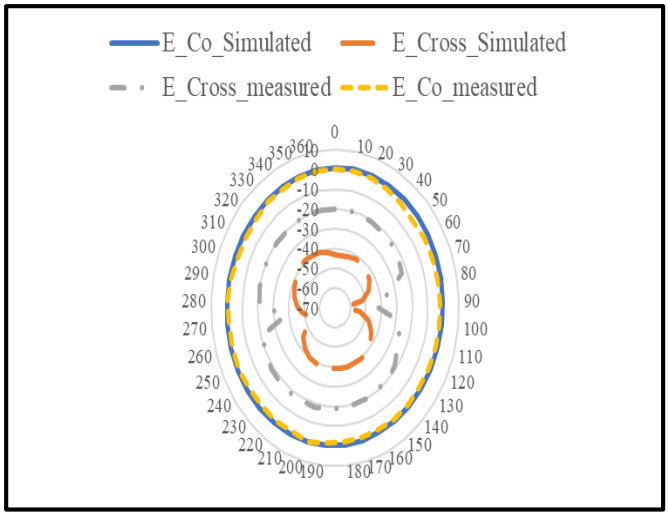

Fig. 10 E-plane co-polarization and cross-polarization plots for the antenna, comparing simulation outcomes with actual measurements

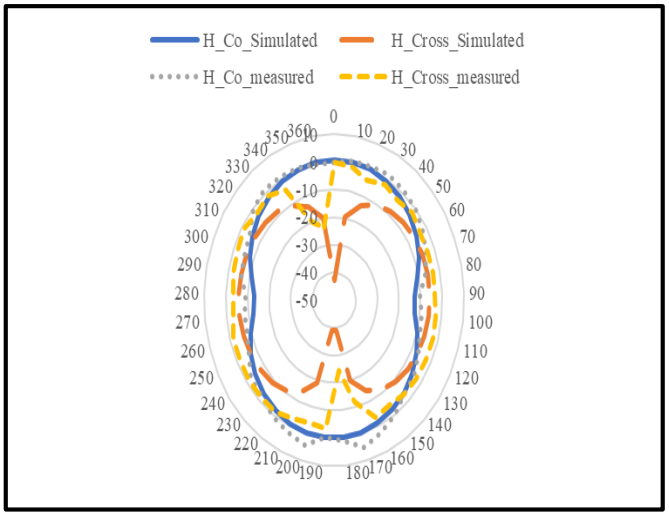

Fig. 11 H-plane co-polarization and cross-polarization plots for the antenna, comparing simulation outcomes with actual measurements

Table 3. Parametric comparative analysis of the textile antenna

Reported literatures	Substrate Material	Resonance Frequency	Size of Antenna	Gain	Design Complexity
[3]	Textile	2.45 GHz	72.4 mm × 65.5 mm	6.2-7.8 dBi	Medium
[4]	Textile	2.4 GHz	30 mm × 20 mm	2.05 dBi	Medium
[19]	Textile	2.45GHz	48 mm × 52 mm	6.84 dBi	High
[20]	Textile	2.45 GHz	140 mm × 70 mm	4.7 dBi	Simple
[21]	Textile	2.45GHz	60 mm × 55 mm	8 dBi	Medium
[7]	Textile	2.45 GHz	41.4 mm × 82.8 mm	7.6 dBi	High
Proposed Design	Textile	2.5 GHz	40.35 mm × 23.57 mm	1.73 dBi	Simple

The parameters include L as the patch length, *λ(0)* as the wavelength in free space, and *ε(eff)* indicating the effective dielectric constant of the substrates involved. Similarly, the resonant frequency of a rectangular microstrip patch antenna was estimated via Equation (2),

$$f(0) = \frac{c}{2L\sqrt{\varepsilon(eff)}} \quad (2)$$

Where $f(0)$ is the resonant frequency, *c* is the speed of light, *L* is the length of the patch, and *ε(eff)* is the effective dielectric constant of the substrates. The input impedance of the microstrip patch antenna was estimated via Equation (3),

$$Z(in) = \frac{jZ(0)\,tan(\beta h)}{1 + jtan(\beta h)} \quad (3)$$

Here, *Z(in)* is the input impedance, *Z(0)* is the feed line's characteristic impedance, h is the thickness of the substrate, and β corresponds to the set of propagation constants. This constant was estimated via Equation (4),

$$\beta = \frac{2\pi}{\lambda(eff)} \quad (4)$$

Where $\lambda(eff)$ is the effective wavelength of the transmission lines. This effective dielectric constant of a microstrip transmission line is calculated via Equation (5),

$$\varepsilon(eff) = \frac{\varepsilon(r)+1}{2} + \left(\frac{\varepsilon(r)-1}{2}\right)\left(1 + \frac{12h}{w}\right)^{-0.5} \quad (5)$$

Where $\varepsilon(r)$ is the relative dielectric constant of the substrate, h is the thickness of the substrate, and w is the width of the transmission lines. Based on these design parameters, the antenna's characteristics were estimated for different input scenarios. Similarly, the SIW variations along with their effects on resonance frequencies were analyzed.

3. SIW Variations and their Effects

The influence of SIW on the patch antenna depends on several factors, including the number, diameter, position, and spacing. To investigate this effect, an analysis was performed by varying the diameter, number, and locations of vias used for SIW. Variations in vias and their effect on the center frequency's sensitivity were depicted in Table 1. It has been observed that, for a fixed operating frequency, higher miniaturization was achieved. By varying the size and number of vias, design experiment 23 resulted in a dual frequency band (at 2.41 and 5.68 GHz) with antenna gain of 1.3dB.

Figures 2, 3, and 4 illustrate the SIW sensitivity analysis to show the dependence of the number, its diameter, and location on the antenna's structure parameters. It has been observed that if the number of vias and their diameter increase, the resonant frequency decreases when positioned close to the patch's feed, while maintaining a return loss below -10dB and an acceptable gain value. Furthermore, by varying the number of vias, the maximum return loss was achieved with six or eight vias.

The analysis demonstrates that incorporating SIW with a patch antenna is an effective strategy that helps in downsizing the antenna, with significant performance implications tied to the vias' count, diameter, and their specific locations. This information is crucial for designing miniaturized antennas with optimal performance for various applications.

Experimental results indicate that the input impedance can be altered by varying the diameter of the vias, thereby enabling multifrequency operation without sacrificing radiation and impedance performance. The reduction in size of the shortened patch generates additional capacitance that counteracts the inductance of the patch. Moreover, loading vias within the patch increases the current path, thereby reducing its size. The symmetrically located vias alter the electric field distribution, leading to a decrease in cross-polarization. The results of the experiments suggest that the antenna design with 12 vias with a diameter of 1 mm and a spacing of 1 mm meets all the constraints imposed on the performance parameters, as depicted in Figure 5.

The simulation result of an antenna loaded with vias as 12, giving a -25.29 dB return loss at a 2.46 GHz resonant frequency, is shown in Figure 6.

4. Fabrication and Performance Evaluation

The miniaturized antenna, designed with SIW, is fabricated on a flexible textile substrate having a dielectric constant of 2.75 and a thickness of 1.5 mm. The fabrication process is successful, and the resulting antenna with measurement setup is presented in Figure 7.

Experiments were conducted in an anechoic environment to evaluate the performance of the manufactured miniature antenna with SIW. The outcomes of these investigations are elaborated upon in this part. Return loss against frequency and gain against frequency for the manufactured flexible antenna featuring shorting posts are displayed in Figure 8 and Figure 9, respectively.

Table 2 contrasts simulated and measured results, offering additional validation of the performance attributes of the antenna design put forth. Figures 10 and 11 depict the plots of the simulated and measured designs for the E-plane co-polarization, E-plane cross-polarization, H-plane co-polarization, and H-plane cross-polarization under various conditions.

The performance of the suggested antenna design does not fall short of the necessary criteria for radiation, despite the fact that there is a tiny discrepancy between the simulated and measured results of the proposed antenna design. It is possible

that the divergence was caused by defects in the soldering and losses in the connection and the coaxial cable. A comparative examination of textile-based antennas reveals trade-offs among substrate material, resonance frequency, antenna size, gain, and design complexity. Notably, the proposed design exhibits a compact size (40.35 mm × 23.57 mm) at 2.5 GHz, indicating effective miniaturization; it has a gain of 1.73 dBi suited for certain wearable applications, contrasting with higher gains (up to 8 dBi) in some comparative studies; the design is simple, facilitating fabrication for wearable/IoT use; most referenced designs operate near 2.4-2.5 GHz for common wireless bands; and textile substrates highlight flexibility and conformability advantageous for wearable integration. Table 3 presents the findings of a comprehensive study on textile antennas that operate in the ISM band, which were reported by various researchers. These findings demonstrate that the suggested design is compact, straightforward, and satisfies the design criteria for on-body applications, with an electrical size of $\lambda/7$ for a variety of different scenarios. Based on this performance, it can be observed that the proposed antenna can be used for a wide variety of real-time scenarios.

5. Conclusion

This paper examines the impact of SIW on flexible antenna performance. SIW can decrease antenna size without sacrificing performance, as per the interpretations after simulations and experiments. The findings indicate that vias' placement, number, and diameter have a major effect on antenna performance. Optimising SIW designs also makes it possible to operate at multifrequency, enhance impedance matching and lessen cross-polarization. The flexible antenna configuration with twelve vias yields a gain of 1 dBi and a return loss of -25.29 dB. The findings give the best insights regarding designing compact flexible microstrip antennas with optimized performance for various applications.

Examining the effects of Substrate Integrated Waveguide (SIW) approaches on microstrip antenna performance reveals exciting directions for future study, such as advanced SIW configuration optimisation that explores the interaction between substrate and parameters for improved miniaturisation. SIW for wideband and multiband operation in cutting-edge applications like satellite communications, 5G, and the Internet of Things (IoT) can also be explored.

References

[1] Bancha Luadang et al., "NFC-Enabled Far-Field Antenna on PET Flexible Substrate for 3G/4G/LTE Mobile Devices," *IEEE Access*, vol. 7, pp. 171966-171973, 2019. [CrossRef] [Google Scholar] [Publisher Link]

[2] Haiying Huang, "Flexible Wireless Antenna Sensor: A Review," *IEEE Sensors Journal*, vol. 13, no. 10, pp. 3865-3872, 2013. [CrossRef] [Google Scholar] [Publisher Link]

[3] Ruben Del-Rio-Ruiz et al., "Reliable Lab-Scale Construction Process for Electromagnetically Coupled Textile Microstrip Patch Antennas for the 2.45 GHz ISM Band," *IEEE Antennas and Wireless Propagation Letters*, vol. 19, no. 1, pp. 153-157, 2020. [CrossRef] [Google Scholar] [Publisher Link]

[4] Adel Y.I. Ashyap et al., "Inverted E-Shaped Wearable Textile Antenna for Medical Applications," *IEEE Access*, vol. 6, pp. 35214-35222, 2018. [CrossRef] [Google Scholar] [Publisher Link]

[5] Heejae Lee, Jinpil Tak, and Jaehoon Choi, "Wearable Antenna Integrated into Military Berets for Indoor/Outdoor Positioning System," *IEEE Antennas and Wireless Propagation Letters*, vol. 16, pp. 1919-1922, 2017. [CrossRef] [Google Scholar] [Publisher Link]

[6] Nurul Husna Mohd Rais et al., "Dual-Band Suspended-Plate Wearable Textile Antenna," *IEEE Antennas and Wireless Propagation Letters*, vol. 12, pp. 583-586, 2013. [CrossRef] [Google Scholar] [Publisher Link]

[7] Feng-Xue Liu et al., "Textile Folded Half-Mode Substrate-Integrated Cavity Antenna," *IEEE Antennas and Wireless Propagation Letters*, vol. 15, pp. 1693-1697, 2016. [CrossRef] [Google Scholar] [Publisher Link]

[8] Sana Ahmed et al., "A Compact Kapton-Based Inkjet-Printed Multiband Antenna for Flexible Wireless Devices," *IEEE Antennas and Wireless Propagation Letters*, vol. 14, pp. 1802-1805, 2015. [CrossRef] [Google Scholar] [Publisher Link]

[9] Shu-Kuan Zhao et al., "A Low-Profile Dielectric Resonator Antenna with Compact-Size and Wide Bandwidth by Using Metasurface," *IEEE Access*, vol. 9, pp. 29819-29826, 2021. [CrossRef] [Google Scholar] [Publisher Link]

[10] Wei Luo, and Ping Wang, "A Compact UHF-RFID Tag Antenna with Embedded AMC for Metallic Objects," *IEEE Antennas and Wireless Propagation Letters*, vol. 22, no. 4, pp. 873-877, 2023. [CrossRef] [Google Scholar] [Publisher Link]

[11] Xiao-Fei Li et al., "Compact Dual-Frequency 2-D Van Atta Array Using the Reconfigurable AMC Antenna," *IEEE Antennas and Wireless Propagation Letters*, vol. 22, no. 12, pp. 3162-3166, 2023. [CrossRef] [Google Scholar] [Publisher Link]

[12] Wentao Li et al., "Compact Inkjet-Printed Flexible MIMO Antenna for UWB Applications," *IEEE Access*, vol. 6, pp. 50290-50298, 2018. [CrossRef] [Google Scholar] [Publisher Link]

[13] Abdulrahman S.M. Alqadami et al., "Compact Unidirectional Conformal Antenna Based on Flexible High-Permittivity Custom-Made Substrate for Wearable Wideband Electromagnetic Head Imaging System," *IEEE Transactions on Antennas and Propagation*, vol. 68, no. 1, pp. 183-194, 2020. [CrossRef] [Google Scholar] [Publisher Link]

[14] Constantine A. Balanis, *Antenna Theory: Analysis and Design*, 4th ed., John Wiley & Sons, Inc., 2016. [Google Scholar] [Publisher Link]

[15] Iqra Aitbar et al., "AMC Integrated Multilayer Wearable Antenna for Multiband WBAN Applications," *Computers, Materials & Continua*, vol. 71, no. 2, pp. 3227-3241, 2022. [CrossRef] [Google Scholar] [Publisher Link]

[16] Girish Kumar, and K.P. Ray, *Broadband Microstrip Antennas*, Artech House, 2002. [Google Scholar] [Publisher Link]

[17] R. Waterhouse, "Small Microstrip Patch Antenna," *Electronics Letters*, vol. 31, no. 8, pp. 604-605, 1995. [CrossRef] [Google Scholar] [Publisher Link]

[18] Supriyo Dey, and Raj Mittra, "Compact Microstrip Patch Antenna," *Microwave and Optical Technology Letters*, vol. 13, no. 1, pp. 12-14, 1996. [CrossRef] [Google Scholar] [Publisher Link]

[19] Mahmoud Wagih et al., "Real-World Performance of Sub-1 Ghz And 2.4 Ghz Textile Antennas for RF-Powered Body Area Networks," *IEEE Access*, vol. 8, pp. 133746-133756, 2020. [CrossRef] [Google Scholar] [Publisher Link]

[20] Ismahayati Adam et al., "Investigation on Wearable Antenna Under Different Bending Conditions for Wireless Body Area Network (WBAN) Applications," *International Journal of Antennas and Propagation*, vol. 2021, pp. 1-9, 2021. [CrossRef] [Google Scholar] [Publisher Link]

[21] Shengjian Jammy Chen et al., "A Robust Snap-on Button Solution for Reconfigurable Wearable Textile Antennas," *IEEE Antennas and Wireless Propagation Letters*, vol. 66, no. 9, pp. 4541-4551, 2018. [CrossRef] [Google Scholar] [Publisher Link]